Fundamental Properties of Mie Resonances in Water Cylinders – TM and TE Case Studies

Jacobsen, Rasmus Elkjær; Arslanagic, Samel; Laurynenka, Andrei

Published in:
Proceedings of URSI EM Theory Symposium

Link to article, DOI:
10.23919/ursi-emts.2019.8931486

Publication date:
2019

Document Version
Peer reviewed version

URSI EM Theory Symposium, EMTS 2019, San Diego, CA, 27– 31 May 2019

Fundamental Properties of Mie Resonances in Water Cylinders – TM and TE Case Studies

Rasmus E. Jacobsen* (1), Samel Arslanagić (2), and Andrei V. Lavrinenko (3)
(1), (3) Department of Photonics Engineering, Technical University of Denmark, Kongens Lyngby, 2800, Denmark,
e-mail: (1) rajac@fotonik.dtu.dk, (3) alav@fotonik.dtu.dk,
(2) Department of Electrical Engineering, Technical University of Denmark, Kongens Lyngby, 2800, Denmark,
e-mail: sar@elektro.dtu.dk

Abstract

All-dielectric metamaterials have recently attracted great attention in the artificial material design. They consist of high permittivity inclusions which enable resonances in sub-wavelength structures. In contrast to optics, several high permittivity materials exist in the microwave range. Among these we find one of the most abundant materials on earth: water. In its liquid state, it offers great tunable dynamic properties that can be used in material design. To this end, we presently examine analytically the so-called Mie resonances in water cylinders. Particular attention is devoted to the ability of such cylinders to support electric and magnetic dipole modes, and how these behave with temperature and frequency. Subsequently, we demonstrate that directive forward and backward patterns can be achieved by specific water cylinders with balanced electric and magnetic dipole responses. The results of this work may be used directly in or as a guideline for metamaterial design as well as for simple, cheap and rather directive antennas.

1. Introduction

The possibility to obtain a variety of permittivity and permeability responses using low-loss high permittivity materials, have made all-dielectric metamaterials (MMs) a favorable choice in artificial material design [1-2]. They enable sub-wavelength Mie resonances in high permittivity inclusions employed in a low index matrix. Recently, water has been proposed as an alternative material for inclusions of all-dielectric MMs and metasurfaces (MSs) at microwave frequencies. With its abundancy, bio-friendliness, inexpensiveness and temperature dependent high permittivity, water offers many advantageous properties [3-7]. It was shown that the response of water-based MMs can be tuned/reconfigured thermally by a simple temperature control of the material [3, 9], chemically [10] and mechanically by rotating partially filled containers or simply by reshaping its volume [3, 11]. In [10], the cylindrical shape made it easy to contaminate the water. Besides the high permittivity, water is quite lossy in a wide frequency range rendering it of great use for broadband MS absorbers [12-13]. A MS composed of 'rod-like' water-elements in a foam material was shown to have high reflection and transmission modulation capabilities through a simple mechanical rotation of the surface [7]. The modulation was improved significantly by stacking several MSs in a multilayer array.

Typically, 2-D and 3-D arrays of water elements are studied numerically. In this work, we investigate Mie resonances in isolated water cylinders illuminated by plane waves of different polarizations (both TM and TE cases will be examined). The canonical problem is treated analytically using the cylindrical wave expansion formulation, which enables us to study fundamental properties and various derived effects of water cylinders. The temperature and frequency variation of the induced dipole resonances is evaluated, and throughout the paper, we discuss the potential of such water cylinders to support both isolated (for MM design) and balanced (for directive antenna design) dipole resonances. We mainly focus on the low frequencies where the losses in water have minimal influence on the resonances, and we show that the two polarizations induce completely different electric dipoles, while their magnetic dipoles have identical magnitudes, but different orientations. The magnetic dipole resonances can be improved in both intensity and isolation by increasing the temperature. Moreover, we show that Kerker's conditions can be satisfied for only the TE polarization at non-resonant frequencies, which results in mainly forward/backward scattering. Throughout the work, the time-factor exp $(j\omega t)$, with ω being the angular frequency and t being the time, is assumed and suppressed.

2. Configuration and analytical expressions

We consider a linearly polarized plane wave with the electric (magnetic) field $\mathbf{E}_P^i$ ($\mathbf{H}_P^i$) incident on a water cylinder of radius r_c situated in a free-space medium, see Figure 1(a). Both TM^z and TE^z polarization states of the incident wave are investigated. A Cartesian coordinate system (x, y, z), and an associated cylindrical coordinate system (r, ϕ, z), is placed with their z-axes coincident with the cylinder axis. The cylinder gives rise to the scattered $(\mathbf{E}_P^s, \mathbf{H}_P^s)$ and internal $(\mathbf{E}_P^w, \mathbf{H}_P^w)$ fields which are easily found through the application of boundary conditions at the cylinder surface $r = r_c$. Their amplitude coefficients are given by [14, Sec. 8.4]

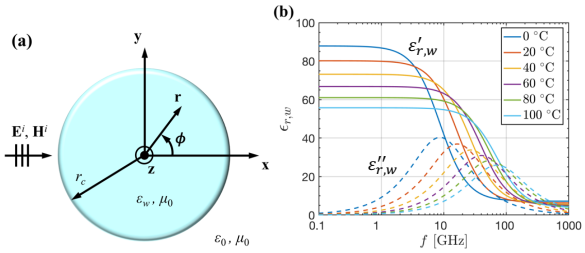

Figure 1. (a) Sketch of the water-sphere in free-space illuminated by a plane wave and **(b)** relative permittvity of water as a function of frequency and temperature.

$$a_n^P = \frac{J_n(k_w r_c) J_n{}'(k_0 r_c) - \alpha_P J_n{}'(k_w r_c) J_n(k_0 r_c)}{\alpha_P J_n{}'(k_w r_c) H_n^{(2)}(k_0 r_c) - J_n(k_w r_c) H_n^{(2)\prime}(k_0 r_c)} \quad (1)$$

$$b_n^P = \frac{J_n{}'(k_0 r_c) H_n^{(2)}(k_0 r_c) - J_n(k_0 r_c) H_n^{(2)\prime}(k_0 r_c)}{\alpha_P J_n{}'(k_w r_c) H_n^{(2)}(k_0 r_c) - J_n(k_w r_c) H_n^{(2)\prime}(k_0 r_c)} \quad (2)$$

respectively, where $P = \mathrm{TM}$ or TE giving $\alpha_{\mathrm{TM}} = \sqrt{\varepsilon_{r,w}}$, or $\alpha_{\mathrm{TE}} = 1/\sqrt{\varepsilon_{r,w}}$. k_w and k_0 are the wavenumbers in water and free-space, respectively, while J_n and $H_n^{(2)}$ are the nth order Bessel function of the first kind and Hankel function of the second kind, respectively. The prime $'$ denotes the derivative with respect to the entire argument.

With the fields at hand, absorption Q_{abs}^P, extinction Q_{ext}^P, and scattering Q_{sca}^P, efficiencies are determined; these are used to describe the response of the water cylinders. In mathematical terms, we have [14, Sec. 3.4]

$$Q_{\mathrm{abs}}^P = Q_{\mathrm{ext}}^P - Q_{\mathrm{sca}}^P \quad (3)$$

where

$$Q_{\mathrm{sca}}^P = \frac{2}{k_0 r_c}\left(|a_0^P|^2 + 2\sum_{n=1}^{\infty}|a_n^P|^2\right) \quad (4)$$

$$Q_{\mathrm{ext}}^P = \frac{2}{k_0 r_c}\mathrm{Re}\left\{a_0^P + 2\sum_{n=1}^{\infty} a_n^P\right\} \quad (5)$$

The induced electric ($\mathbf{p}'_P$ [C]) and magnetic ($\mathbf{m}'_P$ [A·m]) dipole moments per unit length can be determined as [15]

$$\mathbf{p}'_P = \frac{1}{j\omega}\int_S \mathbf{J}_P^d \, ds', \quad \mathbf{m}'_P = \frac{1}{2}\int_S \mathbf{r}' \times \mathbf{J}_P^d \, ds' \quad (6)$$

with $\mathbf{J}_P^d = j\omega\varepsilon_0(\varepsilon_{r,w} - 1)\mathbf{E}_P^w$ being the polarization current density inside the water cylinder, S the cross section of the cylinder, ds' the differential surface element and $\mathbf{r}'$ the position vector. Performing the integrals, one gets for the two polarization cases the following

$$\mathbf{p}'_{\mathrm{TM}} = \hat{\mathbf{e}}_E^{\mathrm{TM}} 2\pi r_c^2 \varepsilon_0(\varepsilon_{r,w} - 1) E_0 b_0^{\mathrm{TM}} \frac{J_1(k_w r_c)}{k_w r_c} \quad (7)$$

$$\mathbf{m}'_{\mathrm{TM}} = \hat{\mathbf{k}}_E^{\mathrm{TM}} \times \hat{\mathbf{e}}_E^{\mathrm{TM}} \pi r_c^3 \omega\varepsilon_0(\varepsilon_{r,w} - 1) E_0 b_1^{\mathrm{TM}} \frac{J_2(k_w r_c)}{k_w r_c} \quad (8)$$

$$\mathbf{p}'_{\mathrm{TE}} = \hat{\mathbf{e}}_E^{\mathrm{TE}} 2\pi r_c^2 \varepsilon_0 \frac{\varepsilon_{r,w} - 1}{\sqrt{\varepsilon_{r,w}}} E_0 b_1^{\mathrm{TE}} \frac{J_1(k_w r_c)}{k_w r_c} \quad (9)$$

$$\mathbf{m}'_{\mathrm{TE}} = \hat{\mathbf{k}}_E^{\mathrm{TE}} \times \hat{\mathbf{e}}_E^{\mathrm{TE}} \pi r_c^3 \omega\varepsilon_0 \frac{\varepsilon_{r,w} - 1}{\sqrt{\varepsilon_{r,w}}} E_0 b_0^{\mathrm{TE}} \frac{J_2(k_w r_c)}{k_w r_c} \quad (10)$$

where $\hat{\mathbf{e}}_E^P$ and $\hat{\mathbf{k}}_E^P$ are the unit vectors of the incident electric field and wave vector, respectively.

In the temperature range from 0 to 100 °C and under normal pressure, water is a liquid. The temperature dependent dielectric permittivity is described by the Debye formula [8]

$$\varepsilon_{r,w}(\omega, T) = \varepsilon'_{r,w} - j\varepsilon''_{r,w} = \varepsilon_\infty(T) + \frac{\varepsilon_s(T) - \varepsilon_\infty(T)}{1 - j\omega\tau(T)} \quad (11)$$

with T [°C] being the temperature of water. $\varepsilon_\infty(T)$ and $\varepsilon_s(T)$ are the optical and static permittivities, respectively, while $\tau(T)$ is the rotational relaxation time. The real ($\varepsilon'_{r,w}$) and imaginary ($\varepsilon''_{r,w}$) parts of (11) are shown in Figure 1(b).

3. Resonant water cylinder

We investigate resonances in a water cylinder with a radius of 10 mm illuminated by z- (TM^z) and y-polarized (TE^z) incident plane waves of amplitudes E_0 [V/m]; both propagate in the $+x$-direction. At a temperature of 20 °C, the absorption and scattering efficiency spectra are shown in Figure 2(a). For validation, the scattering efficiencies calculated in COMSOL Multiphysics is included. For TM^z incidence, the resonance induced at 0.38 GHz is the electric dipole. The magnetic dipole resonance is present for both polarizations at 1.26 GHz and, as shown in Figure 2(b), they have identical magnitudes. Consequently, it follows that $b_0^{\mathrm{TE}} = \sqrt{\varepsilon_{r,w}} b_1^{\mathrm{TM}}$ in (8) and (10), and that the magnitude of the induced magnetic dipole is *polarization insensitive*. This can be used to e.g., separate the magnetic and electric dipole contributions to the efficiencies for TM^z polarization. For TE^z at 2.02 GHz, there is an electric dipole resonance of a very low magnitude; this is partly due to the presence of other resonances, but also due to water losses.

There is an interesting point around 2 GHz for TM^z, where the scattering efficiency has a minimum, while there is a peak in absorption. The minimum is caused by the second harmonic (peak) of the $n = 0$ mode, where $\mathbf{p}'_{\mathrm{TM}}$ has a minimum. The increase in absorption comes from the electric quadrupole resonance ($n = 2$).

The total electric field normalized by the incident field is shown in Figure 2(c) and (d) in the xy-plane at 1.26 GHz (magnetic dipole) for TM^z and TE^z, respectively. The field profiles are very different even though they exhibit magnetic dipoles of equal magnitudes, which is due to the difference in their orientations and the presence of other resonances for TM^z as shown in Figure 3. This is also why the scattering and absorption efficiencies are different. The scattering efficiency is highest for $\mathbf{p}'_{\mathrm{TM}}$, while the

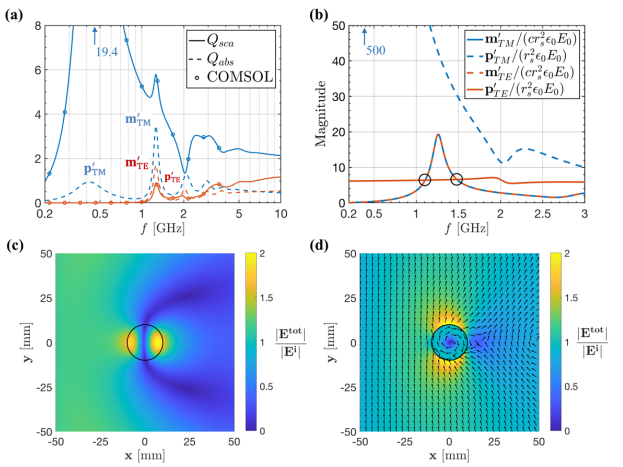

Figure 2. (a) the absorption and scattering efficiencies as a function of frequency f (logarithmic scale) for both TM^z (blue) and TE^z (red) polarization; **(b)** the magnitude of the normalized induced magnetic and electric dipole moments as a function of frequency f; the total electric field normalized with the incident field at $f = 1.26$ GHz in the xy-plane for **(c)** TM^z and **(d)** TE^z polarizations. The arrows indicate the direction of the electric field. The cylinder radius is in all cases set to $r_c = 10$ mm.

absorption is most profound for $\mathbf{m}'_{\mathrm{TM}}$. However, $\mathbf{m}'_{\mathrm{TE}}$ is more isolated making it more suitable for e.g., MMs. Absorbed power in a dielectric is given by $P_{\mathrm{abs}} = 0.5\omega\varepsilon_0\varepsilon''_{r,w}\int_V |\mathbf{E}_P^w|^2\, dv$; thus the high absorption is related to high internal field intensities and small losses. If the losses are too high, the induced dipoles will be affected by it. This absorbed energy results in the heating of water.

Isolation of dipole resonances plays an important role in MM design in particular. The isolation of the induced dipoles is shown in Figure 3 by the magnitude of the internal coefficients for their first and second modes. The first resonance ($n = 0$) is clearly better isolated compared to the second ($n = 1$) for both polarizations.

The temperature variation is investigated for the scattering efficiency as well as for $\mathbf{p}'_{\mathrm{TM}}$ and $\mathbf{m}'_{\mathrm{TE}}$ (remember $\mathbf{m}'_{\mathrm{TM}}$ and $\mathbf{m}'_{\mathrm{TE}}$ are identical except for their orientations). The intensity of $\mathbf{p}'_{\mathrm{TM}}$ decreases with increasing temperature causing a lower scattering efficiency, while opposite behavior is observed for the other induced dipoles. This is due to the change in water's permittivity: at low

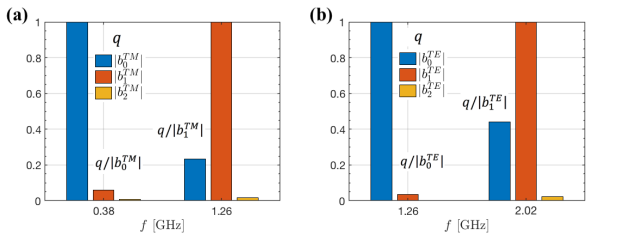

Figure 3. Isolation of resonances shown by internal coefficients at the magnetic and electric dipole resonance frequencies with $T = 20$ °C in **(a)** TM^z and **(b)** TE^z.

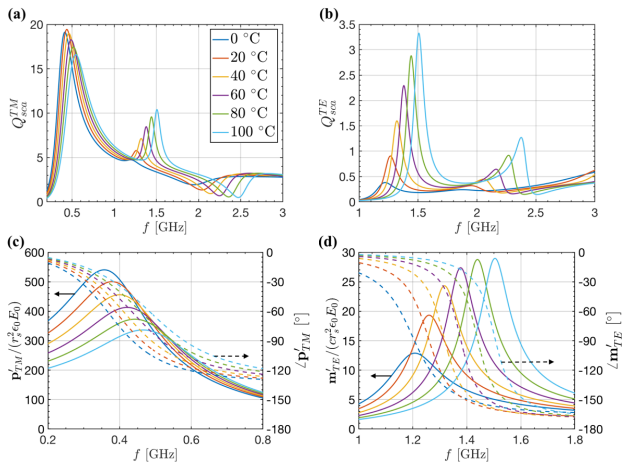

Figure 4. The temperature and frequency variation of the scattering efficiency for **(a)** TM^z and **(b)** TE^z cases, as well as the dipole moments **(c)** $\mathbf{p}'_{\mathrm{TM}}$ and **(d)** $\mathbf{m}'_{\mathrm{TE}}$ **.** In all cases, the cylinder radius is set to $r_c = 10$ mm.

frequencies $\varepsilon''_{r,w}$ decreases only slightly with increasing temperature, while $\varepsilon'_{r,w}$ decreases significantly causing the blue-shift. At even higher frequencies, an increase in temperature will have a more profound effect on the efficiencies. In general, the dipole resonance frequencies are blue-shifted by approximately 25 % with an increase of temperature from 0 to 100 °C. The losses in water must be minimized in order to achieve pronounced and isolated resonances if water inclusions are to be used in MMs and MSs. Generally, this is achieved at low frequencies and/or high temperatures.

Several ways to maximize scattering in one direction have been proposed, e.g. one considers pairing dipoles and quadrupoles [16]. We next show that it is possible to attain directed scattering by satisfying the so-called Kerker's conditions in the examined water cylinders. The dipole moments shown in Figure 2(b) and 3(c)-(d) are normalized as $\mathbf{m}'/(c{r_s}^2\varepsilon_0 E_0)$ and $\mathbf{p}'/({r_s}^2\varepsilon_0 E_0)$, where c is the speed of light, since the difference in their units is [m/s]. In the case of $m'/p' = c$ (where $\mathbf{p}' = \hat{\mathbf{e}}_E p'$ and $\mathbf{m} = \hat{\mathbf{k}}_E \times \hat{\mathbf{e}}_E m'$), the scattering will be maximized in the forward direction, while if $m'/p' = -c$, it will be in the backward direction. The frequencies, where these conditions are met, are marked by the black circles in Figure 2(b) for TE^z. In Figure 5, the normalized differential scattering width [14, Sec. 3.4] is shown at these frequencies as well as at the magnetic dipole resonance frequency. The orientations of the dipoles are drawn for each frequency. Such effects are interesting for MMs, MSs and directive antennas designs, since only forward (backward) scattering corresponds to zero reflection (transmission). TM^z polarization does not exhibit any cases with the required conditions due to the strong electric dipole. For enhanced scattering in one direction, one could consider tilting the cylinder to enhance the electric dipole moment. A different shape exhibiting greater induced dipole moments (or higher order modes) could also be pursued.

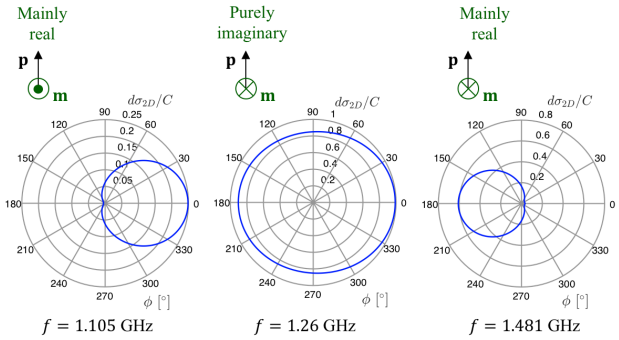

Figure 5. Normalized differential scattering width for TE^z at 1.105, 1.26 and 1.481 GHz.

4. Conclusions

The electromagnetic response of a water cylinder resonating around 1 GHz was investigated for both TM^z and TE^z polarization states of the incident wave. The analytical expressions for the scattering and absorption efficiencies as well as the magnetic and electric dipole moments were outlined in Section 2. The two polarization states result in two different electric dipoles, while their magnetic dipole moments are identical except for their orientations. The TM^z case lead to a profound electric dipole at very low frequencies, while for the TE^z case, the magnetic dipole was the most pronounced resonance. Both of these were the only well-isolated resonance, while all other modes were influenced by other resonances. Increasing the temperature resulted in more profound and isolated magnetic resonances, which are desirable features for prospective MM and MS designs. For TM^z incidence, the temperature increase had a negative influence on the electric dipole resonance at very low frequencies. At last, we showed that balanced magnetic and electric dipole moments, (Kerker's conditions), were achievable for the TE^z incidence, while the electric dipole was too intense in the TM^z case. These conditions resulted in primarily forward or backward scattering. These effects are of interest in various areas of artificial materials and electrically small and directive antennas.

5. References

1. S. Jahani, and Z. Jacob, "All-dielectric metamaterials," Nat. Nanotechnol., **11**, pp 23–36, 2016.

2. J. Sauter, I. Staude, M. Decker, E. Rusak, D. N. Neshev, I. Brener, and Y. S. Kivshar, "Active tuning of all-dielectric metasurfaces," ACS Nano, vol. 9, no. 4, 2015.

3. A. Andryieuski, S. M. Kuznetsova, S. V. Zhukovsky, Y. S. Kivshar, and A. V. Lavrinenko, "Water: promising opportunities for tunable alldielectric electromagnetic metamaterials," Sci. Rep., **5**, 13535, 2015.

4. Y. J. Yoo et al., "Metamaterial absorber for electromagnetic waves in periodic water droplets," Sci. Rep., **5**, 14018, 2015.

5. X. Cai, S. Zhao, M. Hu, J. Xiao, N. Zhang, and J. Yang, "Water based fluidic radio frequency metamaterials", J. Appl. Phys., **122**, 184101, 2017.

6. M. A. Gorlach, M. Song, A. P. Slobozhanyuk, A. A. Bogdanov, and P. A. Belov, "Topological transition in coated wire medium". Phys. Status Solidi RRL, **10**, 2016, pp 900-904.

7. R. E. Jacobsen, A. V. Lavrinenko and S. Arslanagić, "Water-Based Metasurfaces for Effective Switching of Microwaves," IEEE Antennas Wirel. Propag. Lett., **17**, 4, 2018, pp 571-574.

8. W. Ellison, "Permittivity of pure water, at standard atmospheric pressure, over the frequency range 0-25 thz and the temperature range 0-100 c," J. Phys. Chem. Ref. Data, **36**, 2007, pp 1–18.

9. M. V. Rybin, D. S. Filonov, P. A. Belov, Y. S. Kivshar, and M. F. Limonov, "Switching from Visibility to Invisibility via Fano Resonances: Theory and Experiment," Sci. Rep., **5**, 8774, 2015.

10. X. Yang et al., "Reconfigurable all-dielectric metasurface based on tunable chemical systems in aqueous solution," Sci. Rep., **7**, 3190, 2017.

11. M. Odit, P. Kapitanova, A. Andryieuski, P. Belov, and A. V. Lavrinenko, "Experimental demonstration of water based tunable metasurface," Appl. Phys. Lett., **109**, 011901, 2016.

12. J. Ren, and J. Y. Yin. "Cylindrical-Water-Resonator-Based Ultra-Broadband Microwave Absorber," Optical Materials Express **8**, 8, 2018, pp. 2060–2071.

13. Q. Song et al., "Water- Resonator-Based Metasurface: An Ultrabroadband and Near-Unity Absorption," Adv. Opt. Mater., **5**, 1601103, 2017.

14. C. F. Bohren, and D. R. Huffman, "Absorption and Scattering of Light by Small Particles," Wiley, 1983.

15. A. Dirksen, S. Arslanagic, and O. Breinbjerg, "Resonances and dipole moments in dielectric, magnetic and magnetodielectric cylinders – an overview," Appl. Phys. A, **103**, 2011.

16. R. Alaee, R. Filter, D. Lehr, F. Lederer, C. Rockstuhl, "A generalized Kerker condition for highly directive nanoantennas," Opt. Lett, **40**, 11, 2015, pp. 2645-2648.